B-Physics and Quarkonia studies with early ATLAS data

Erez Etzion [*] [a] on behalf of the ATLAS Collaboration
November 2009.

[a]Tel Aviv University, Raymond and Beverly Sackler school of Physics and Astronomy.
Tel Aviv 69978, Israel

Quarkonia and B-Physics are among the first areas to be investigated with the first data collected by ATLAS. The ATLAS detector at CERN's LHC is preparing to take data from proton-proton collisions expected to start by the end of 2009. Investigation of the decay of B-hadrons represents a complementary approach to direct searches for physics beyond the Standard Model. Early B-Physics data will provide valuable information on the detector performance, as well as allow calibration studies in support of New Physics searches. Meaningful quarkonia studies performed with early data are expected to have the reach to make authoritative statements about the underlying production mechanism and provide cross-sections in this new energy regime. We review various aspects of prompt quarkonium production at the LHC: the accessible ranges in transverse momentum and pseudo-rapidity, spin alignment of vector states, separation of color octet and color singlet production mechanism and feasibility of observing radiative χ_c decays.

1. Introduction and motivations

The main goal of ATLAS [1], one of the general purpose Large Hadron Collider (LHC) experiments, is looking for signals of New Physics beyond the Standard Model (BSM). While the expected BSM signatures are mostly at high transverse momenta (p_T), the B-Physics processes are concentrated in the low p_T region. Nevertheless ATLAS is able to provide B-Physics measurements based on its precise vertexing and tracking, its muon identification and a dedicated trigger strategy. The LHC is expected to produce a large number of B decays and heavy quarkonia states such as J/ψ and Υ in the low luminosity runs during the first few years of running. Their sizable branching fraction into charged lepton pairs allows for easy separation of these events from the expected huge hadronic background. The ATLAS efforts concentrate on those B decays that can be selected by the first and second trigger levels. The most favorable B and heavy quarkonium trigger signatures will be events decaying to

μ pair, either directly or via a J/ψ meson. Using the J/ψ trigger ATLAS will be able to collect unprecedentedly high statistics of $B_s \rightarrow J\psi\phi$ decays, allowing measurements of CP violating effects, which are predicted by some BSM models to be significantly larger than the SM prediction. The di-muon trigger will also give ATLAS access to potentially large numbers of rare $B_s \rightarrow \mu\mu$ decays. Exclusive decay channels of B^+ and B_d^0 with two muons in the final state, will be measured for studying mass and lifetime as well as production cross-section. Being narrow resonances, the quarkonia are perfectly suited for alignment and calibration of the ATLAS trigger and tracking systems. On top of that, understanding the details of the prompt charmonium production is a challenging task and a good testbed for various QCD calculations, spanning both perturbative and non-perturbative regimes through the creation of heavy quarks in the hard process and their subsequent evolution into physical bound states.

2. ATLAS B-Physics di-muon trigger

ATLAS uses a fast and efficient muon based B-Physics triggering strategy. The LHC will col-

lide two 7 TeV proton beams at a rate of 40 MHz, which together with pile-up will result in an interaction rate of up to around 1 GHz. The ATLAS trigger acts to reduce this rate to around 100 Hz in three successive levels, whilst keeping only events 'of interest'. The trigger first level (level-1) decision is based on coarse granularity of two sub-detector systems: the muon trigger chambers and the calorimeters. The second level trigger (level-2) receives from level-1 data restricted to limited Regions of Interest (RoI). For a level-1 muon, the level-2 will use the information from the muon and inner detector tracking chambers to improve the muon momentum estimate, which allows a tighter selection based on this quantity. There are two specific types of trigger dedicated to quarkonium: one which requires two level-1 RoIs corresponding to two muon candidates with p_T values above thresholds of 4 and 6 GeV respectively, and the other requires a single level-1 RoI above a threshold of 4 GeV and searches for the second muon of opposite charge in a wide RoI at level-2. A complementary trigger on J/ψ events is triggering on a single higher p_T (10 GeV) muon and searching for a matched track at the off-line analysis level. Before incorporating trigger and reconstruction efficiencies, the predicted cross-sections for $pp \rightarrow J/\psi \rightarrow \mu^+\mu^- + X$ were calculated for a number of p_T thresholds on the di-muon trigger (see Table 1 for details). Figure 1 illustrates the distribution of cross-sections across the values of the p_T of the harder and softer muon from the quarkonium decay without any muon cuts applied and zero polarization. The lines overlaid on the plots represent the muon trigger thresholds $p_T > 6$ GeV and $p_T > 4$ GeV for the harder and the software muon respectively (denoted further by "6+4 GeV" or $\mu6\mu4$). Similarly "4+4 GeV" ($\mu4\mu4$) refers to the trigger threshold $p_T > 4$ GeV applied on both muons. The "10+0.5 GeV" ($\mu10$) refers to trigger p_T threshold of 10 GeV applied on one of the muons only. In all cases the pseudorapidity, η, of a muon lies within an interval $|\eta| < 2.5$.

Even if the bulk of the J/ψ are produced under the trigger thresholds, nevertheless, due to the high cross-section the number of accepted J/ψ will be substantially larger than at the Tevatron.
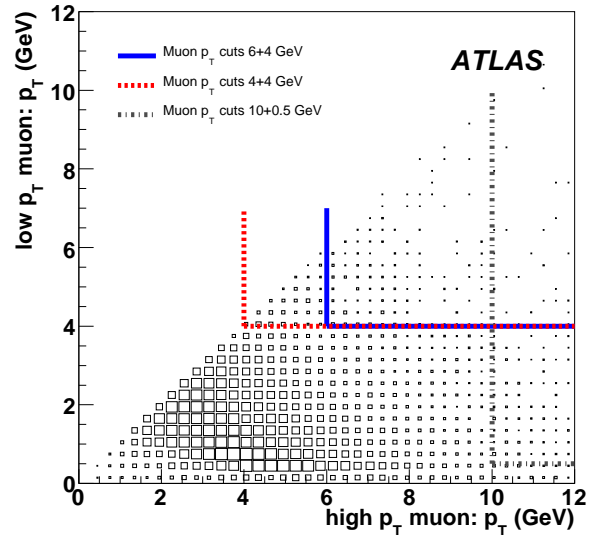

Figure 1. Density of J/ψ production cross-section as a function of the hardest and softer muon p_T of muons coming from J/ψ. No cut was placed on the generated sample, but the overlaid lines represent the thresholds of observed events with trigger cuts applied.

In the Υ case, due to it's relatively larger mass the bulk of the production is in the region near the muon threshold of 5 and 4 GeV. This means that by lowering the threshold for the higher momentum muon we can significantly increase the number of recorded Υ events.

Estimated quarkonia cross-sections for the three scenarios are presented in Table 1. The production will be dominated by J/ψ and $\Upsilon(1S)$. while ψ' and $\Upsilon(2S)$, $\Upsilon(3S)$ are expected to give smaller contributions.

Precise cross-section measurements require a good understanding of the event and trigger selection efficiency. To evaluate the trigger efficiency we use tag-and-probe (TAP) method applied on the real J/$\psi \rightarrow \mu^+\mu^-$ data. In the TAP method a single triggered muon from a reconstructed di-muon decay of an identified specific particle is

Table 1
Predicted cross sections for various quarkonium states into muons, for different pt thresholds (before trigger and reconstruction efficiencies). The last column shows the overlap between the di-muon and single muon samples.

Quarkonium	Cross-section, nb			
	$\mu4\mu4$	$\mu6\mu4$	$\mu10$	$\mu6\mu4$ and $\mu10$
pp→J/ψ	28	23	23	5
pp→ ψ'	1.0	0.8	0.8	0.2
pp→ $\Upsilon(1S)$	48	5.2	2.8	0.8
pp→ $\Upsilon(2S)$	16	1.7	0.9	0.3
pp→ $\Upsilon(3S)$	9.0	1.0	0.6	0.2

used as a tagged muon while we probe the trigger efficiency of the second muon. We verified that the efficiency derived with the TAP method on simulated events is in good agreement with the single muon trigger efficiency directly estimated from Monte Carlo samples.

3. B-Physics early measurements

The large production cross section of $b\bar{b}$ events will enable, even during the initial low luminosity phase of the LHC, the observation of various exclusive channels such as $B^+ \rightarrow J/\psi K^+$, $B_d \rightarrow J/\psi K^0$ or $B_s \rightarrow J/\psi \phi$. The measurement of the known properties of the B hadrons such as masses and lifetime will be used to study and tune the detector. The known channels will serve as a reference while searching for the rare B decays.

The charmonium events and the B decays to J/ψ share a similar detection strategy. In any event which passes the di-muon trigger, all the reconstructed muon candidates are combined into oppositely charged pairs, and each of these pairs is analyzed in turn. The invariant mass of the combined muons is required to be within a defined window around the J/ψ mass. In the direct charmonium search, if the invariant mass of the two muons is above 1 GeV, we first attempt to refit the tracks to a common vertex. If a good vertex fit is achieved, the pair is accepted for further analysis. If the invariant mass of the refitted tracks is within 300 MeV for J/ψ or 1 GeV for Υ

(six times the expected average mass resolution) of the expected mass, the pair is considered as a charmonium candidate.

The radial displacement of the two-track vertex from the beamline is used to distinguish between prompt J/ψ originated at the proton proton interaction and the B-hadron decays into quarkonia. The pseudo-proper decay time, τ, is defined as

$$\tau = \frac{L_{xy} \cdot M_{J/\psi}}{p_T(J/\psi)}, \tag{1}$$

where $M_{J/\psi}$ and $p_T(J/\psi)$ represent the J/ψ invariant mass and transverse momentum, and L_{xy} is the transverse decay length of the meson. The resolution in the pseudo-proper decay time is expected to vary from 0.110 ps for the low p_T charmonia down to 0.07 ps for the higher p_T. As demonstrated in Figure 2 a cut on this quantity can efficiently distinguish between prompt and indirect J/ψ events.

In the case of $B^+ \rightarrow J/\psi K^+$ all tracks with positive charge which do not originate from the primary vertex are considered as K^+. We fit the three tracks corresponding to a J/ψ and the K^+ candidates to a common vertex. The momentum sum of the two has to point to the primary vertex. A maximum likelihood (ML) method is used to fit the B^+ mass distribution taking Gaussian probability density function for the signal and linear distribution for the background. The mass resolution in this channel is estimated, for an integrated luminosity of 10 pb^{-1} to be $\sigma = 42.2 \pm 1.3$ MeV with a total efficiency of $29.8 \pm 0.8\%$. The differential cross-section is obtained in this channel in different bins of $p_T(B^+)$ using the number of the signal events and the efficiency from the ML fit to the invariant mass distribution. The total cross-section is determined with the same procedure but for the whole p_T region of B^+. For an integrated luminosity of 10 pb^{-1}, we determined that the total production cross section can be measured with a statistical precision better than 5% and the differential cross-section can reach a precision of 10%. The systematic uncertainties are expected to be dominated by the luminosity and the branching ratio.

The channel $B_s \rightarrow J/\psi \phi$ has the potential to reveal New Physics signals. The weak mixing
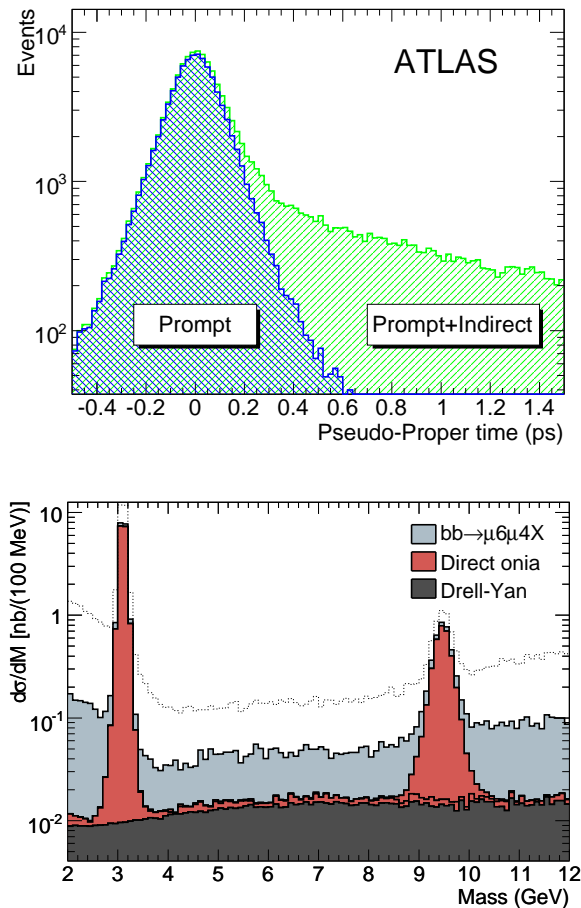
Figure 2. Upper - Pseudo-proper decay time, τ, distribution for reconstructed prompt J/ψ (cross-hatched, centred at zero) and the sum of prompt and indirect J/ψ from B-decays (hatched, exponential distribution).

Lower - Sources of low invariant mass di-muons, reconstructed with a $\mu6\mu4$ p_T trigger, with the requirement that both muons are identified as coming from a primary vertex and with a pseudo-proper decay time smaller than 0.2 ps. The white area represents the background that was rejected with the pseudo-proper decay time treatment.

phase ϕ_s, which in the SM is very small, may be enhanced by BSM processes. The time dependent angular distribution of this decay depends on seven physics parameters: two independent complex transversely amplitudes, the mean lifetime and the mass eigenstate width difference ($\Delta\Gamma$), and the weak mixing phase. The full analysis will require a fit to these parameters and is sensitive to statistics, experimental resolution of lifetime, mass and decay angles as well as flavour tagging performance and background rejection. The experience of the Tevatron experiments taught us that a few thousands events only allow a two dimensional profile likelihood fit in ϕ_s-$\Delta\Gamma$ plane. The LHC after the high luminosity runs will enable a simultaneous determination of all seven parameters. With early data the ATLAS program will begin with calibration measurements supporting this analysis. The topological identical channel $B_d \rightarrow J/\psi K^0$, which is expected to yield 15 times more statistics, is the the primary background but is also an essential as a control sample. It will allow high precision tests of the lifetime measurement as well as flavour tagging analysis calibration. With the earliest data, ATLAS will use a fit to simultaneously access the mean mass and lifetime of the B_s and the B_d mesons. This will enable the testing of our understanding of the tracking at low p_T scale after 150 pb^{-1}, and will start to improve the world precisions on these measurements after about 1 fb^{-1}. Early on, topologically similar backgrounds will be admitted to the analysis and secondary vertex cuts will not be applied. After 10 fb^{-1} the precision on the B_d lifetime is expected to be 10% and similar precision for the B_s mean lifetime is expected after 150 pb^{-1}.

4. Charmonium analysis

Charmonium production comprises of three main processes: direct singlet production, octet production and singlet production of χ states. Each of these processes is characterized by different differential cross-sections, $\frac{d\sigma}{dp_T}$.

The reconstruction efficiency of charmonium varies with p_T and η. When the $p_T(J/\psi) > 10$ GeV we get a sharp rise in its acceptance. The

rise in the Υ case is less sharp and it reaches a high acceptance level around 30 GeV. Both channels reach a similar plateau at acceptance of around 85%. The trigger requires both muons to pass the p_T threshold and so the angular separation between the two muons is not large for most of the accepted events. We describe the opening angle by $\delta R = \sqrt{\delta\phi^2 + \delta\eta^2}$, where $\delta\phi$ and $\delta\eta$ are the differences in the azimuthal angle and the pseudorapidity of the two muons from J/ψ. Typical values for δR are ≈ 0.47 which means that requiring both muons to be above the p_T threshold forces them to fly very close one to each other. For this reason the J/ψ angular acceptance follows closely the individual muon distribution and its dependence on material and detector effects. In the Υ case, due to its higher mass, it tends to be produced with higher p_T. Therefore the separation angle δR is much wider, the muons do not go to the same area in the detector and the efficiency dependence on pseudorapidity is much smoother than in the J/ψ case. The main sources of low invariant mass di-muons expected to dominate the background for prompt charmonium are: decays in flight of $\pi^\pm$ and $K^\pm$ (which are reduced after cuts to below the 1% level); di-muon production via the Drell-Yan process (which are rendered essentially negligible by the trigger requirements); continuum of muon pairs from beauty (and charm) decays and the main source - indirect J/ψ production - the reduction of which is discussed below.

All the background sources apart from the Drell-Yan pairs contain muons which do not originate from the interaction point, and this is used to suppress their contamination by rejection of the events containing a secondary vertex if identified. As detailed in the previous section a cut on the pseudo-proper decay time is used to distinguish between the direct and indirect charmonium cases. Figure 2 shows the pseudo-proper decay time distribution of the two samples and the impact on the mass distribution when rejecting events with a pseudo-proper time above 0.2 ps.

Using the $\mu 10$ trigger each reconstructed single muon candidate is combined with oppositely-charged tracks reconstructed in the same event within a cone of $\delta R = 3.0$. Any track, including those that were not identified as muons, are examined. As in the di-muon analysis, we require that both the identified muon and the track are flagged as having come from the primary vertex. In addition, we impose a cut on the transverse impact parameter d_0, $|d_0| < 0.04$ mm on the identified muon and $|d_0| < 0.10$ mm on the second track, in order to further suppress the number of background pairs from B-decays. We obtain a J/ψ invariant mass resolution close to that in those events passing the trigger requiring both muons to be confirmed. It's worth noting that the signal-to-background ratio around the J/ψ peak improves slightly with increasing transverse momentum of J/ψ. At higher p_T the $\cos\theta^*$ acceptance also becomes broader, which should help independent polarization measurements.

ATLAS is capable of detailed checks of the predictions of various models describing the evolution of heavy quark antiquark pair into a quarkonium bound state. Among the models which are considered are: Color Evaporation Model (CEM) [2], the Color Singlet Model (CSM) [3] which failed to predict the J/ψ production rate measured by CDF, and the Nonrelativistic QCD (NRQCD) Colour Octet Model (COM) [4] which was proposed to explain this discrepancy. The good description of the Tevatron data by the COM model shown in Figure 3 is at least in part due to the tuning of some of its parameters which were determined from the same data. However, the difference between the CDF measurement of J/ψ polarization dependence on transverse momentum (p_T) and the theory predictions (Figure 4) is motivating us to repeat the measurement in the LHC's higher energy and luminosity regime.

The polarization of quarkonia can be measured using the angular distribution of the daughter particles produced in the decay.

$$\frac{d\Gamma}{d\cos\theta^\star} \propto 1 + \alpha\cos^2\theta^\star, \qquad (2)$$

where $\cos\theta^\star$ is the angle between the direction of the positive (by convention) muon from quarkonium decay in the quarkonium rest frame, and the direction of the quarkonium itself in the lab-
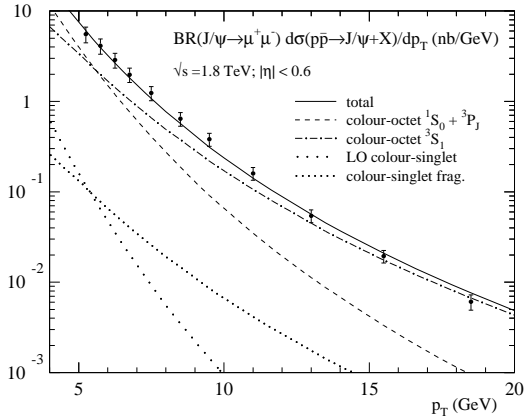
Figure 3. Differential cross-section of J/ψ production at CDF with theoretical predictions for color-singlet and color-octet model production [6]

Figure 4. Polarization of J/ψ production as a function of p_T at CDF, (data points), curves for limit cases of the k_T factorization model, and a band for NRQCD predictions (from [7]).

oratory frame. The polarization parameter α, defined as $\alpha = (\sigma_T - 2\sigma_L)/(\sigma_T + 2\sigma_L)$, is equal to $+1$ for transversely polarized quarkonia production (helicity ± 1). σ_T and σ_L are the transverse and longitudinal cross sections. For longitudinal (helicity 0) polarization, α is equal to -1. Unpolarized production consists of equal fractions of helicity states $+1$, 0 and -1, and corresponds to $\alpha = 0$.

The previous Tevatron measurements were limited to below around 20 GeV, where the polarization is best predicted and the theory most understood. At ATLAS we aim to measure the polarization of directly produced prompt quarkonium in the p_T region up to ~ 50 GeV and beyond with extended coverage in $\cos\theta^\star$. This will allow for improved fidelity of efficiency, provide better discrimination of longitudinal and transverse polarizations and therefore reduced systematic uncertainties.

Evidently the polarization measurement can significantly suffer from low $|\cos\theta^\star|$ acceptance, and hence from difficulties in separating detector efficiency corrections from polarization state ef-
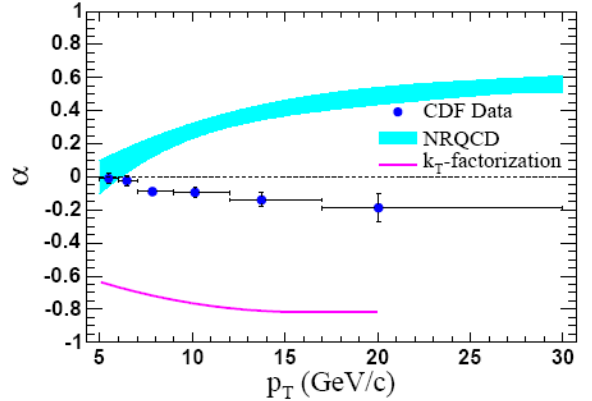
fects. The di-muon trigger requirement for both muons to be above a certain p_T threshold ($\mu6\mu4$) reduces to a minimum the acceptance at large values of $|\cos\theta^\star|$, where the difference between various polarization states is the more pronounced (see for example the two polarization states on the lower plots of Figure 5). The acceptance of the single muon trigger sample ($\mu10$) is very different. Here the efficiency is higher at large values of $|\cos\theta^\star|$ and drops around zero. Figure 5 (on the top) demonstrates how the two samples complement each other mainly at the low p_T regions, while at high p_T the two triggers increasingly overlap, thus allowing for a cross-check of acceptance and efficiency corrections. The p_T distributions of both samples, $\mu6\mu4$ and $\mu10$ events, were appropriately combined. The combined distribution $dN^{\mathrm{raw}}/d\cos\theta^*$, was corrected according to equation 3,

$$\frac{dN^{\mathrm{cor}}}{d\cos\theta^*} = \frac{1}{\mathcal{A}(p_T, \cos\theta^*) \cdot \varepsilon_1 \cdot \varepsilon_2} \cdot \frac{dN^{\mathrm{raw}}}{d\cos\theta^*}. \quad (3)$$

Here ε_1 stands for the trigger and reconstruction efficiency, while ε_2 denotes the efficiency of background suppression cuts for each sample, and $\mathcal{A}(p_T, \cos\theta^*)$ is the kinematic acceptance of the

trigger selection. The results obtained when fitting an unpolarized sample ($\alpha = 0$) with statistics corresponding to 10 pb^{-1} are: $\alpha = 0.156 \pm 0.166, -0.006 \pm 0.032, 0.004 \pm 0.029, -0.003 \pm 0.037, -0.039 \pm 0.038$ and 0.019 ± 0.057 corresponding to the p_T bins as in Figure 5. The precision of the cross-section derived from the normalization factor are ± 4.35 in the first slice and decreasing from ± 0.09 to ± 0.04 with increasing p_T slices. Repeating the same study with Υ we get back numbers that are consistent with ($\alpha = 0$) but with larger errors running from ± 0.17 to ± 0.22. To further check the ability to measure the polarization we reweighted our raw Monte Carlo (MC) distribution to emulate a transversely polarized ($\alpha = +1$) and a longitudinally polarized ($\alpha = -1$) J/ψ samples. The same analysis was repeated and the results can be seen on the bottom of Figure 5.

A complementary method for polarization measurement has been examined as well [5]. Here a linear combination of three MC generated samples representing longitudinally polarized, transversely polarized and unpolarized events were fitted to the angular distribution of the data. The measured values of α in bins of p_T were well concentrated around the initial value of the polarization that was set in the MC-data sample.

5. Analysis of χ production

A sizeable fraction of prompt J/ψ and Υ are expected to originate from radiative decays of heavier states, χ_c and χ_b. These states have even C parity and therefore have a strong coupling to the color-singlet two gluon state. About 30 to 40% of J/ψ in our signal will come from decays of $\chi_c \rightarrow J/\psi + \gamma$. Unfortunately, the energies of these photons tend to be quite small, and the ability of ATLAS to detect these photons and resolve various χ states is rather limited. For χ_c reconstruction, each selected quarkonium candidate is combined with every reconstructed and identified photon candidate in the event, and the invariant mass of the $\mu\mu\gamma$ system is calculated. The $\mu\mu\gamma$ system is considered to be a χ candidate, if the difference between the invariant masses of the $\mu\mu\gamma$ and $\mu\mu$ systems lies between 200 and

800 MeV, and the cosine of the opening angle between the J/ψ and γ is larger than 0.97.

We fitted three guassians to the difference in invariant masses of the $\mu\mu\gamma$ and $\mu\mu$ measured in those χ candidates. The MC input amplitudes of the peaks were reproduced reasonably well [5]. The overall χ_c reconstruction efficiency is estimated to be about 4%.

6. Physics reach with early ATLAS data

The ATLAS B-Physics program will run from the earliest days and will pursue indirect searches for New Physics via B-hadrons decays. An efficient, fast and clean di-muon trigger scheme will allow ATLAS to collect large samples of B-hadrons and quarkonia throughout the lifetime of the experiment. Reconstruction of exclusive B-meson decays with two muons in the final state, especially with J/ψ, is foreseen already with the first pb^{-1}. Early B-Physics data will provide valuable information on the detector performance and will allow calibration studies in support of New Physics searches. Meaningful quarkonium studies performed with early data are expected to have a sufficient reach to make authoritative statements about the underlying production mechanism and provide cross-section measurements in this new energy regime. Quarkonium spin-alignment measurements at ATLAS will have the capability to distinguish between various production models of quarkonium. Even in the early stages ATLAS is expected to provide competitive measurements of the J/ψ and Υ polarization - p_T dependent values. With several million J/$\psi \rightarrow \mu\mu$ decays, and better understanding of the detector, $\chi_c \rightarrow J\psi\gamma$ should become observable.

REFERENCES

1. G. Aad et al., "The ATLAS Experiment at the CERN Large Hadron Collider", JINST **3:S08003** 2008.
2. J.F. Amundson et al., "Quantitative Tests of Color Evaporation: Charmonium Production", Phys. Lett. **B390**, (1997) 323.
3. See e.g. V. G. Kartvelishvili, A. K. Likhoded, S. R. Slabospitsky, Sov. J. Nucl. Phys. **28**

(1978) 280; M. Gluck, J. F. Owens and E. Reya, "Gluon Contribution To Hadronic J/ψ Production," Phys. Rev. D **17** (1978) 2324; V. G. Kartvelishvili, A. K. Likhoded, Sov. J. Nucl. Phys. **39** (1984) 298.

4. G.T. Bodwin, E. Braaten , G.P. Lepage, "Rigorous QCD Analysis of Inclusive Annihilation and Production of Heavy Quarkonium", Phys. Rev. **D 51**, (1995) 1125, Erratum ibid. D55, (1997) 5853.

5. The ATLAS Collaboration, G. Aad et al., "Expected perfromance of the ATLAS Experiment: Detector, Trigger and Physics", CERN-OPEN-2008-20, arXiv:0901.0512v4; E. Etzion for the ATLAS Collaboration, "ATLAS reach for quarkonium production and polarization measurement", Nucl. Phys. Proc. Suppl. **187** (2009) 136.

6. M. Kramer, "Quarkonium production at high-energy colliders," Prog. Part. Nucl. Phys. **47** (2001) 141.

7. A. Abulencia *et al.* [CDF Collaboration], "Polarization of J/ψ and ψ_{2S} mesons produced in $p\bar{p}$ collisions at $\sqrt{s} = 1.96$-TeV," Phys. Rev. Lett. **99** (2007) 132001.
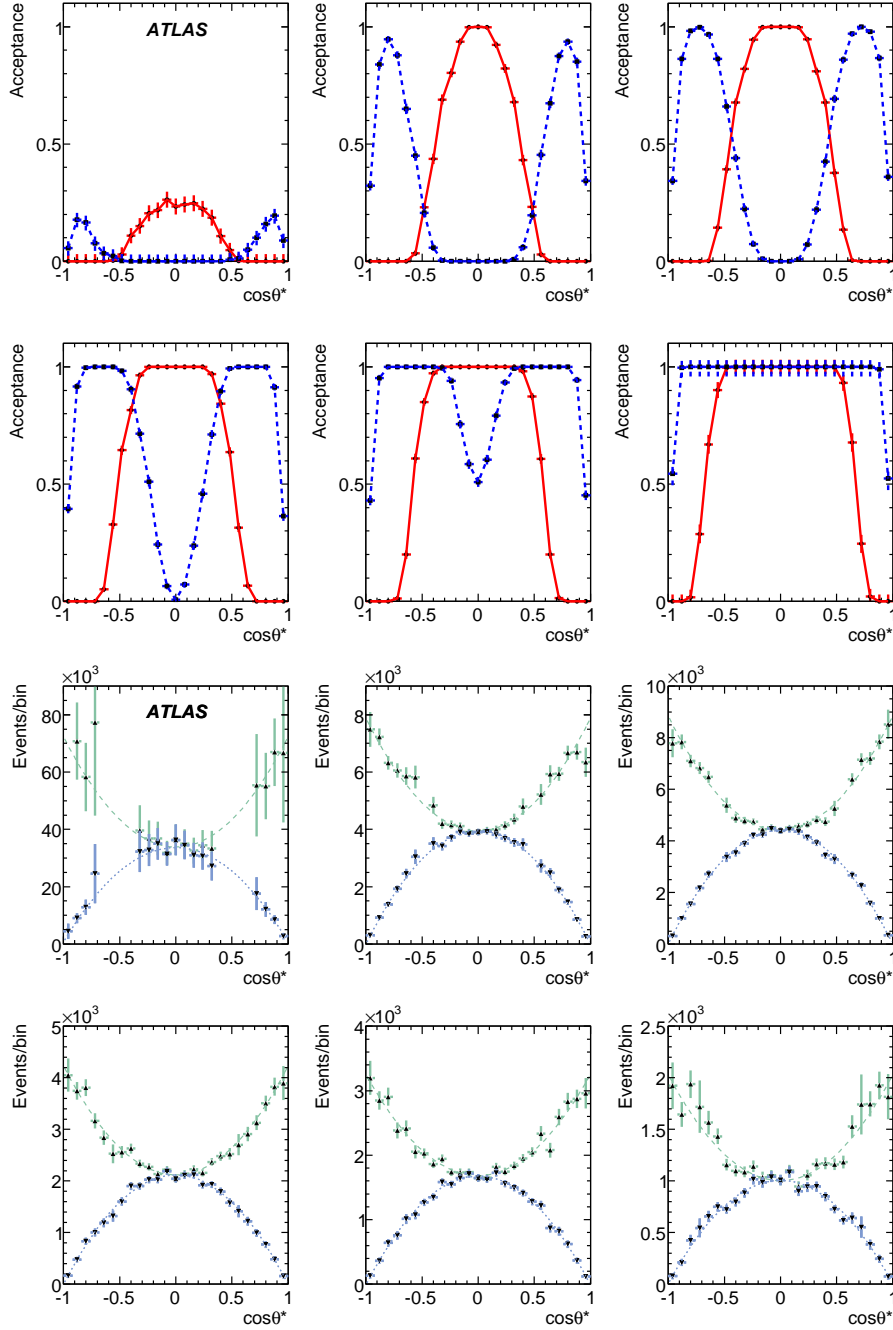
Figure 5. Six figures at the top show kinematic acceptances of the $\mu6\mu4$ (solid line) and $\mu10$ (dashed lines) generator level cuts, calculated with respect to the sample with no generator level cuts on muon p_T, in slices of J/ψ transverse momentum: left to right, top to bottom 9-12 12-13, 13-15, 15-17, 17-21, above 21 GeV.

Six bottom figures show combined and corrected (equation 3) distributions in polarization angle, for longitudinally (dotted lines) and transversely (dashed lines) polarized J/ψ sample in the same p_T slices with statistics corresponding to an integrated luminosity of 10 pb^{-1}.